M. Ramzan[1] / M. Bilal[2] / Jae Dong Chung[3]

Soret and Dufour Effects on Three Dimensional Upper-Convected Maxwell Fluid with Chemical Reaction and Non-Linear Radiative Heat Flux

[1] Department of Computer Science, Bahria University, Islamabad, Pakistan
[2] Department of Mathematics, Capital University of Science and Technology, Islamabad, Pakistan, E-mail: me.bilal.786@gmail.com
[3] Department of Mechanical Engineering, Sejong University, Seoul 143-747, Korea

Abstract:
Three dimensional chemically reactive upper-convected Maxwell (UCM) fluid flow over a stretching surface is considered to examine Soret and Dufour effects on heat and mass transfer. During the formulation of energy equation, non-linear radiative heat flux is considered. Similarity transformation reduces the partial differential equations of flow problem into ordinary differential equations. These non-linear differential equations are then solved by using bvp4c MATLAB built-in function. A comparison of the present results with the published work is also included. Effects of some prominent parameters such as Soret and Dufour number, chemical reaction parameter, Prandtl number, Schmidt number and thermal radiation on velocity, temperature and concentration are discussed graphically and numerically. A comparison with the previously published work is also included in a tabular form.

Keywords: chemical reaction, upper-convected Maxwell fluid, Soret and Dufour effects, non-linear thermal radiation

DOI: 10.1515/ijcre-2016-0136

1 Introduction

Dufour, for the first time pointed out the energy flux generation by composition gradient. This effect is called Dufour effect or diffusion thermal effect. Similarly, the distribution of mass flux due to temperature gradient was defined by Soret and this effect was named as Soret effect or thermo diffusion (Hayat et al. 2015). It is noted that both of these effects can be neglected because of their small order of magnitude, in the study of heat and mass transfer when these are compared with Fourier's law or Fick's law which relates energy and mass flux with temperature and concentration gradient respectively. However when the temperature and concentration gradient are high, these effects are of very significant and can not be neglected. Moreover when the chemical species are introduced at the surface of the fluid (having low density) surrounding by another fluid (having high density), then thermodiffusion and diffusion thermal effects are useful (Makinde and Olanrewaju 2011). These effects are also very important for separation of isotopes and mixture of gases with the high/medium molecular weight (N_2, air) and lighter molecular weight (H_2, He)(Eckert and Drake). Using the Kinetic theory of gases, Soret and Dufour effects have been developed by Chapman and Cowling and Hirshfelder, Curtis, and Bird (1954). Some relevant studies of Soret and Dufour effects are made (see (Hayat et al., 2016a; Hayat et al., 2016a; Mingchun et al., 2013; Ojjela & Kumar, 2016; Reddy, Varma & Kumar, 2016; Ren & Chan, 2016) and refs. therein).

Chemical reaction and thermal radiation have public importance such as plasma wind tunnels, combustion of fossil fuels, electric space crafts propulsion, photo ionization and geophysics. Chemical reaction may be of first order or high order. They may be heterogenous, homogenous, exothermic or endothermic. Many researchers have considered chemical reaction on diverse areas such as combustion (Chaudhary and Merkin 1995), polymer melt flow (Merkin and Mahmood 1998), geophysics (Beg et al. 2013), geothermics (Beg et al. 2007), solar collectors (Steinfeld and Palumbo 2001), and PEM fuel cells (Chia 2006). Uddin et al. (2015) studied about the chemical reaction on magneto-nanofluid for free convection fluid. Convective heat transfer over a wedge for the nanofluid with the effects of chemical reaction, heat generation/absorption and suction was considered by Kasmani et al. (2016).

M. Bilal is the corresponding author.
©2017 by De Gruyter.

Brought to you by | University of Sussex Library
Authenticated
Download Date | 3/1/17 5:03 PM

Fluids which are described by non-linear relationship between stress and shear rate of deformation are known as non-Newtonian fluids. Drilling mud, ceramics, oils and grease, tooth paste, paints and bloods are some common examples of non-Newtonian fluids. These fluids can be classified differential type or rate type fluids. The rheological equations of rate-type fluids are quite complicated as compared to differential type fluids. Viscoelastic fluids such as Oldroyed-B fluid or upper-convected Maxwell fluid are rate-type fluids. Sadeghya, Hajibeygi, and Taghavia (2006) considered upper-convected Maxwell fluid with stagnation point flow. Abel et al. (2012) studied about magnetohydrodynamic upper-convected Maxwell fluid flow for heat transfer over a stretching sheet. Boundary layer flow of Maxwell fluid over a porous shrinking sheet was analyzed by Chapman and Cowling (1940). Heat transfer analysis is carried out by Ali et al. (2016) in a channel using Oldroyd-B fluid in the presence of magnetic field. They used finite difference method to solve the nonlinear differential equations. In another article, Mushtaq et al. (2016a) finds the numerical solution of upper-convected Maxwell fluid using Cattaneo-Christov heat flux model. Some recent study on non-Newtonian fluids can be seen in Ref.(Hayat et al., 2016b; Hayat et al., 2016b; Ramzan & Bilal, 2015; Ramzan & Bilal, 2016; Ramzan et al. 2016).

In the present work non-linear thermal radiation for the upper-convected Maxwell fluid on a bidirectional stretching sheet is considered. Soret and Dufour effects along with chemical reaction are also taken into account. MATLAB built-in bvp4c function is used to investigate the behaviour of different physical parameters on velocity, temperature and concentration profiles. Further a comparison with the previously published work is tabulated and are found in a very good agreement.

2 Mathematical formulation

Three dimensional upper-convected Maxwell fluid flow due to stretching surface in xy-plane is considered. Further, non-linear thermal radiation along with Soret and Dufour effects and chemical reaction of first order homogenous reaction are considered. $U_w(x) = ax$ and $V_w(y) = by$ be the velocities considered on bidirectional stretching surface in x and y directions respectively. T_w and C_w are the constant temperature and concentration on the surface wall. T_∞ and C_∞ denote the faraway temperature and concentration of the fluid where the boundary layer thickness is neglected as shown in Figure 1. The basic equations of the described problem for velocity, temperature and concentration with the assumption of Rosseland approximation can be expressed as (Awais et al., 2014; Liu & Andersson, 2008).

$$\frac{\partial u}{\partial x} + \frac{\partial v}{\partial y} + \frac{\partial w}{\partial z} = 0, \tag{1}$$

$$u\frac{\partial u}{\partial x} + v\frac{\partial u}{\partial y} + w\frac{\partial u}{\partial z} + \lambda_1 \left(\begin{array}{c} u^2\frac{\partial^2 u}{\partial x^2} + v^2\frac{\partial^2 u}{\partial y^2} + w^2\frac{\partial^2 u}{\partial z^2} + \\ 2uv\frac{\partial^2 u}{\partial x \partial y} + 2uw\frac{\partial^2 u}{\partial x \partial z} + 2vw\frac{\partial^2 u}{\partial y \partial z} \end{array} \right) = v\frac{\partial^2 u}{\partial z^2}, \tag{2}$$

$$u\frac{\partial v}{\partial x} + v\frac{\partial v}{\partial y} + w\frac{\partial v}{\partial z} + \lambda_1 \left(\begin{array}{c} u^2\frac{\partial^2 v}{\partial x^2} + v^2\frac{\partial^2 v}{\partial y^2} + w^2\frac{\partial^2 v}{\partial z^2} + \\ 2uv\frac{\partial^2 v}{\partial x \partial y} + 2uw\frac{\partial^2 v}{\partial x \partial z} + 2vw\frac{\partial^2 v}{\partial y \partial z} \end{array} \right) = v\frac{\partial^2 v}{\partial z^2}, \tag{3}$$

$$u\frac{\partial T}{\partial x} + v\frac{\partial T}{\partial y} + w\frac{\partial T}{\partial z} = \alpha_m\frac{\partial^2 T}{\partial z^2} - \frac{1}{\rho c_p}\frac{\partial q_r}{\partial z} + \frac{D_m k_T}{C_s c_p}\frac{\partial^2 C}{\partial z^2}, \tag{4}$$

$$u\frac{\partial C}{\partial x} + v\frac{\partial C}{\partial y} + w\frac{\partial C}{\partial z} = D_m\frac{\partial^2 C}{\partial z^2} + \frac{D_m k_T}{T_m}\frac{\partial^2 T}{\partial z^2} - K_1\left(C - C_\infty\right). \tag{5}$$

Brought to you by | University of Sussex Library
Authenticated
Download Date | 3/1/17 5:03 PM

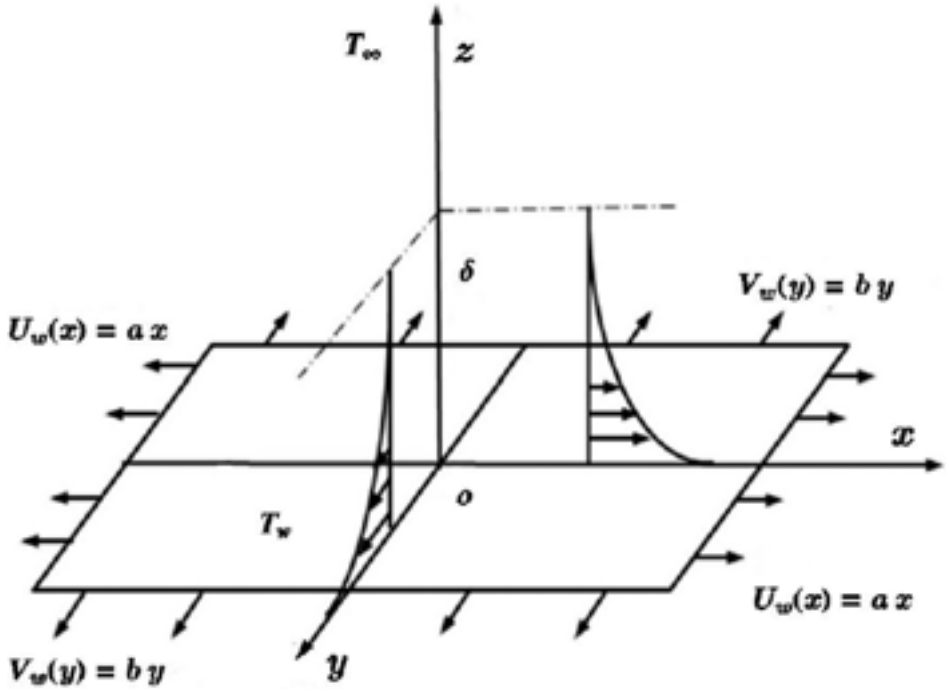

Figure 1: Geometry of the problem.

The corresponding boundary conditions for the governing PDEs are

$$\begin{gathered} u = U_w = ax,\ v = V_w = by,\ w = 0,\ T = T_w,\ C = C_w \text{ at } z = 0, \\ u, v \to 0,\ T \to T_\infty,\ C \to C_\infty \text{ as} z \to \infty \end{gathered} \tag{6}$$

We, now, introduce the following dimensionless variables:

$$\begin{gathered} u = axf'(\eta),\ v = ayg'(\eta),\ w = -\sqrt{av}\,(f(\eta) + g(\eta)), \\ \theta(\eta) = \frac{T - T_\infty}{T_w - T_\infty},\ \phi(\eta) = \frac{C - C_\infty}{C_w - C_\infty},\ \eta = \sqrt{\frac{a}{\nu}}z, \end{gathered} \tag{7}$$

In eq. 4, q_r is Rosseland radiative heat flux (Mushtaq et al. 2016b), defined as

$$q_r = -\frac{4\sigma^*}{3k^*}\frac{\partial T^4}{\partial z}. \tag{8}$$

In this study, as we are considering non-linear thermal radiation, so T in eq. 7 can be expressed as

$$T = T_\infty\left((\theta_w - 1)\,\theta + 1\right), \tag{9}$$

using eq. 9 into eq. 8, we obtain

$$q_r = -\frac{16\sigma^*}{3k^*}T_\infty^3\left((\theta_w - 1)\,\theta + 1\right)^3\frac{\partial T}{\partial z}, \tag{10}$$

where $\theta_w = \frac{T_w}{T_\infty}$ is the temperature ratio parameter.

Equation 1 is identitically satisfied while eqs (2)–(5) are converted to the following ordinary differential equations:

$$f''' - f'^2 + (f+g)f'' + K\left(2f'\left(f+g\right)f'' - (f+g)^2 f'''\right) = 0, \tag{11}$$

$$g''' - g'^2 + (f+g)g'' + K\left(2g'\left(f+g\right)g'' - (f+g)^2 g'''\right) = 0, \tag{12}$$

$$\left(1 + \frac{4}{3}Rd(1 + (\theta_w - 1)\,\theta)^3\right)\theta'' + 4Rd\,(\theta_w - 1)\,(1 + (\theta_w - 1)\,\theta)^2\theta'^2$$

$$+Pr\left(f+g\right)\theta' + PrDu\phi'' = 0 \tag{13}$$

Brought to you by | University of Sussex Library
Authenticated
Download Date | 3/1/17 5:03 PM

$$\phi'' + Sc\left(f+g\right)\phi' + SrSc\theta'' - Sc\gamma\phi = 0. \tag{14}$$

The transformed boundary conditions are:

$$\begin{gathered} f\left(0\right)=0,\ f'\left(0\right)=1,\ g\left(0\right)=0,\ g'(0)=c,\ \theta\left(0\right)=1,\ \phi\left(0\right)=1, \\ f'\left(\infty\right)\to 0,\ g'\left(\infty\right)\to 0,\ \theta\left(\infty\right)\to 0,\ \phi\left(\infty\right)\to 0. \end{gathered} \tag{15}$$

Different dimensionless parameters appearing in eqs (11)–(15) are defined as

$$\begin{gathered} K=\lambda_1 a,\ Pr=\frac{\nu}{\alpha}=\frac{\rho c_p \nu}{k},\ Rd=\frac{4\sigma^* T_\infty^3}{kk^*},\ \theta_w=\frac{T_w}{T_\infty},\ c=\frac{b}{a}, \\ Sc=\frac{\nu}{D_m},\ Sr=\frac{D_m k_T(T_w-T_\infty)}{T_m\nu(C_w-C_\infty)},\ \gamma=\frac{k}{a},\ Du=\frac{D_m k_T(C_w-C_\infty)}{C_s c_p \nu(T_w-T_\infty)}. \end{gathered} \tag{16}$$

The important quantities of interest are local Nusselt and Sherwood numbers are defined as

$$Nu_x=\frac{xq_w}{k\left(T_w-T_\infty\right)},\qquad Sh_x=\frac{xj_w}{D_m\left(C_w-C_\infty\right)}. \tag{17}$$

Here, heat and mass fluxes are defined as

$$q_w=-k\left(\frac{\partial T}{\partial z}\right)_{z=0},\qquad j_w=-D_m\left(\frac{\partial C}{\partial z}\right)_{z=0}. \tag{18}$$

The dimensionless form of Local Nusselt number and Sherwood number are:

$$Re_x^{-1/2}Nu_x=-[1+4/3Rd\theta_w^3]\theta'\left(0\right),\qquad Re_x^{-1/2}Sh_x=-\phi'\left(0\right). \tag{19}$$

3 Solution methodology

The resulting ordinary differential equations and their respective boundary conditions obtained after applying similarity transformation are solved by a MATLAB built-in function bvp4c for various values of different parameters. On the basis of a number of computational experiments, we are considering [0, 8] as the domain of the problem instead of (0, ∞) as there is no noticeable variation in the results after 8. We denote f by y_1, g by y_4, θ by y_7 and ϕ by y_9 for converting the boundary value problem (BVP) (11)-(15) to the following initial value problems (IVPs) consisting of 10 first order differential equations.

$$\begin{aligned}
&y_1' = y_2 && y_1(0)=0,\\
&y_2' = y_3 && y_2(0)=1,\\
&y_3' = \frac{1}{1-K\left(y_1+y_4\right)^2}\left[y_2^2-\left(y_1+y_4\right)y_3-2Ky_2y_3\left(y_1+y_4\right)\right] && y_3(0)=r,\\
&y_4' = y_5 && y_4(0)=0,\\
&y_5' = y_6 && y_5(0)=c,\\
&y_6' = \frac{1}{1-K\left(y_1+y_4\right)^2}\left[y_5^2-\left(y_1+y_4\right)y_6-2Ky_5y_6\left(y_1+y_4\right)\right] && y_6(0)=s,\\
&y_7' = y_8 && y_7(0)=1,\\
&y_8' = \frac{-1}{1+4/3Rd\left(1+\left(\theta_w-1\right)y_7\right)^3}\left[\begin{array}{c}4Rd\left(\theta_w-1\right)\left(1+\left(\theta_w-1\right)y_7\right)^2y_8^2+\\ \Pr\left(y_1+y_4\right)y_8+\Pr Duy_{10}'\end{array}\right] && y_8(0)=t,\\
&y_9' = y_{10} && y_9(0)=1,\\
&y_{10}' = -Sc\left(y_1+y_4\right)y_{10}-ScSry_8' + Sc\gamma y_9 && y_{10}(0)=p.
\end{aligned} \tag{20}$$

4 Results and discussions

To visualize the effect of different physical parameters on velocities $f'(\eta)$, $g'(\eta)$, temperature $\theta(\eta)$ and concentration profiles $\phi(\eta)$, Figures (2)–(19) are plotted. In all these computations, we have considered $Du = 0.1$, $Sc = 0.5$, $Pr = 3.0$, $K = 1.0$, $Rd = 1.0$, $\theta_w = 1.5$, $c = 0.5$, $Sr = 0.2$, $\gamma = 0.1$.

Brought to you by | University of Sussex Library
Authenticated
Download Date | 3/1/17 5:03 PM

Figure 2 and Figure 3 reflects the behaviour of Deborah number K which is a ratio of fluid relaxation time to its characteristic time scale on velocity profile. When the shear stress is applied on the fluid then the time in which it gain its equilibrium position is called relaxation time. This time is higher for the fluids having high viscosity, so increase in Deborah number may increase in viscosity of the fluid and hence the velocity decreases as shown in Figure 2 and Figure 3. When K is increased, the hydrodynamic boundary layer thickness decreases. Figure 4 and Figure 5 shows the variation of Deborah number K on temperature and concentration profiles. It is observed that temperature increases with an increase in relaxation time. From this observation, we can conclude that elastic force promotes the heat transfer in upper-convected Maxwell fluid. The similar behaviour is observed for the concentration profile in Figure 5, in which mass transfer increases with an increase in Deborah number.

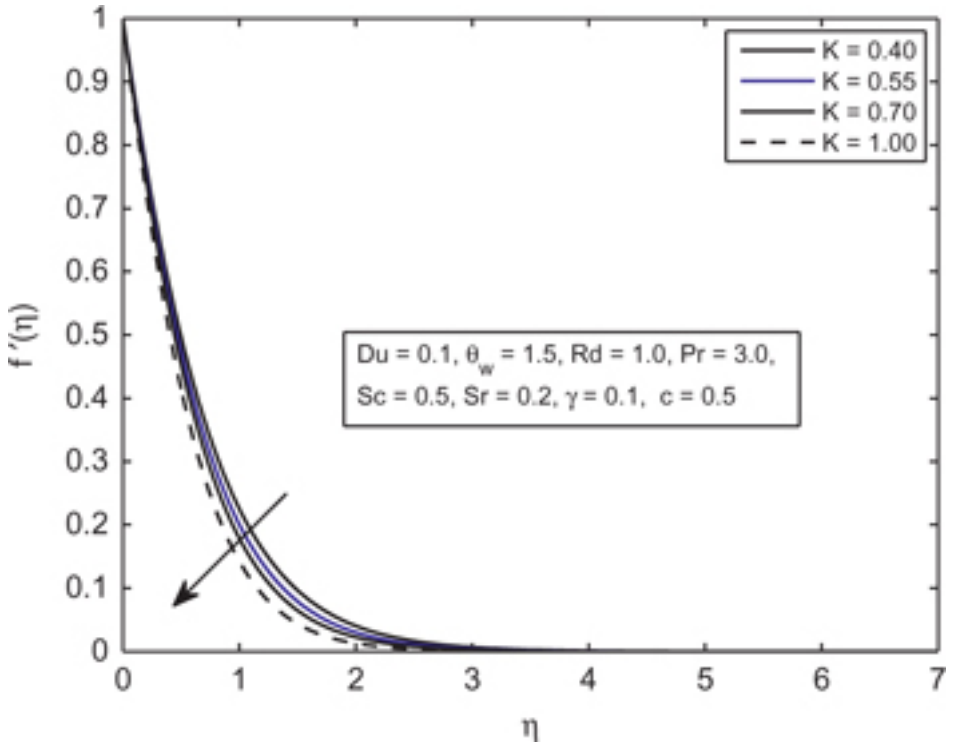

Figure 2: Influence of K on f'.

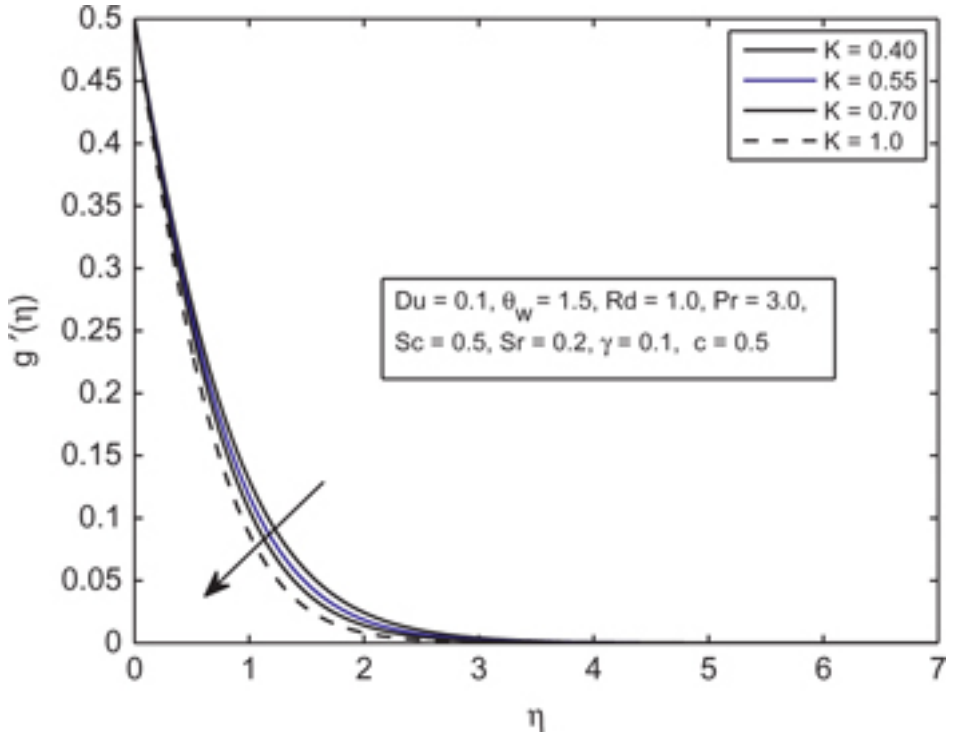

Brought to you by | University of Sussex Library
Authenticated
Download Date | 3/1/17 5:03 PM

Figure 3: Influence of K on g'.

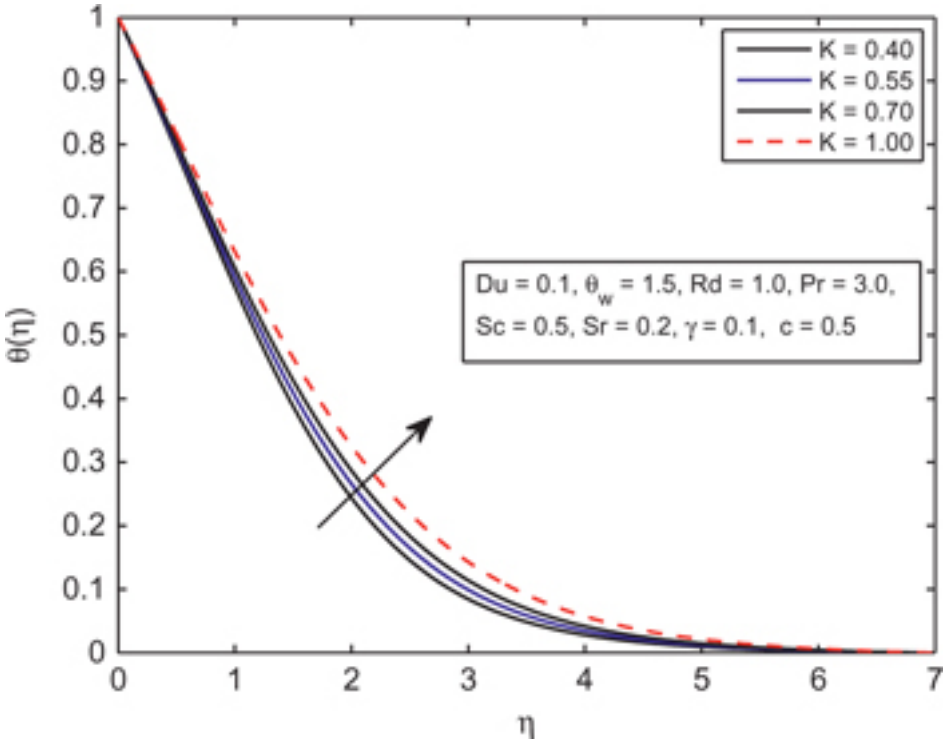

Figure 4: Influence of K on θ.

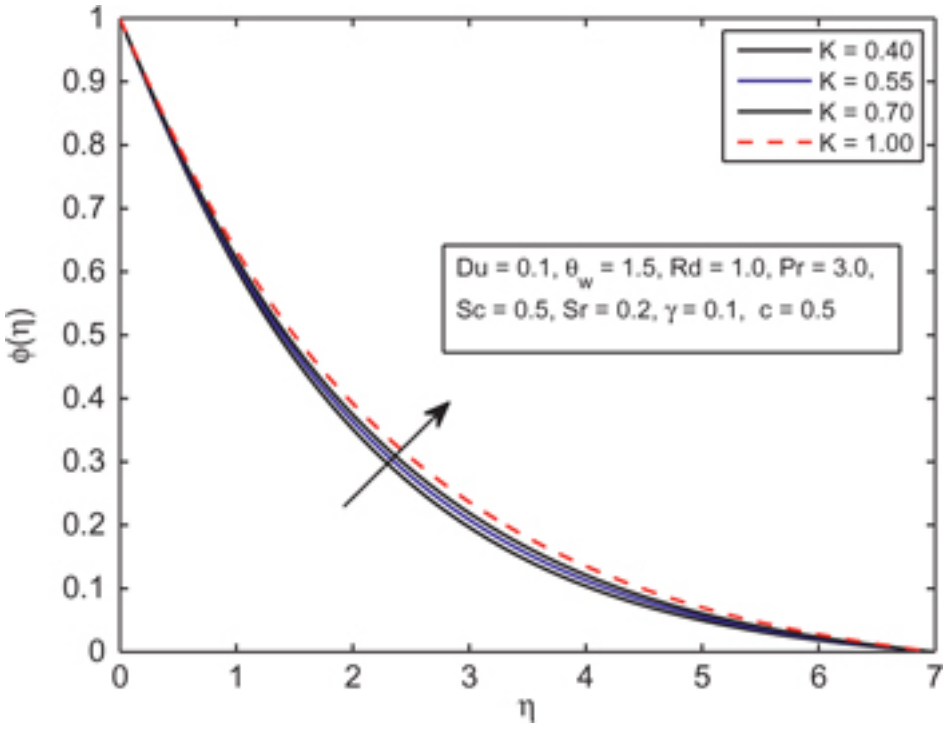

Figure 5: Influence of K on ϕ.

In Figure 6–Figure 8 the effect of stretching rate ratio c on velocities and temperature profile is shown. An opposite effect of c on velocity profiles in $x-$ and $y-$direction is noticed in Figure 6 and Figure 7. As $c = b/a$, so increment in c means decrement in a, which implies decrease in velocity along x axis. Similarly, increasing value of c means increment in b, which resultantly increase the velocity of the fluid in $y-$direction. From Figure 8, it is seen that temperature decreases with the increasing value of c. The influence of Sr on concentration profile is depicted in Figure 9 which shows increase in concentration profile for the increasing value of Soret number. Figure 1 is plotted to visualize the effect of radiation parameter Rd on temperature profile for linear

Brought to you by | University of Sussex Library
Authenticated
Download Date | 3/1/17 5:03 PM

and non-linear cases. Figure shows that temperature increases for both cases. It is also noticeable that profile merge for small value of *Rd* however the difference grows up for linear and non-linear radiation when *Rd* is increased. In Figure 11 the variation of θ_w is studied for the temperature profile. From the figure, it is observed that temperature enhanced for the increasing value of temperature ratio parameter θ_w.

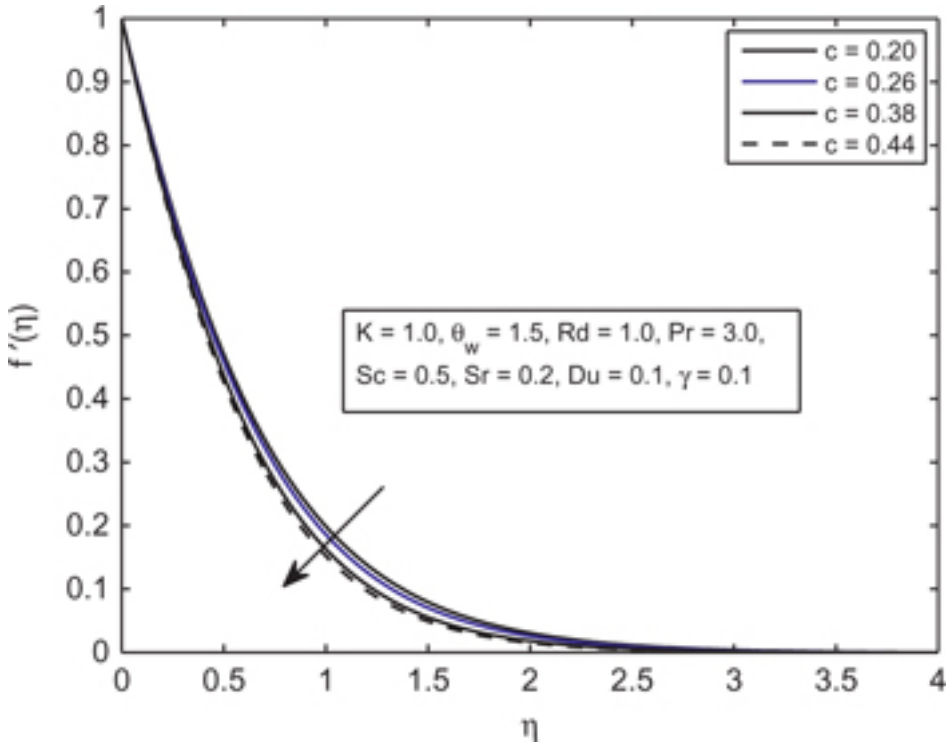

Figure 6: Influence of c on f'.

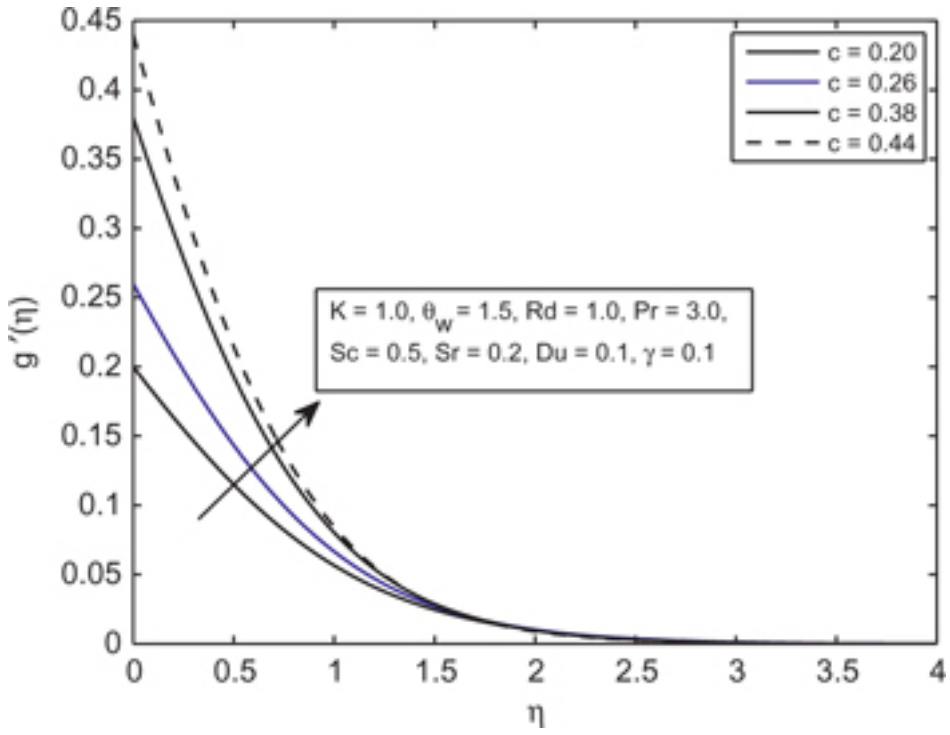

Figure 7: Influence of c on g'.

Brought to you by | University of Sussex Library
Authenticated
Download Date | 3/1/17 5:03 PM

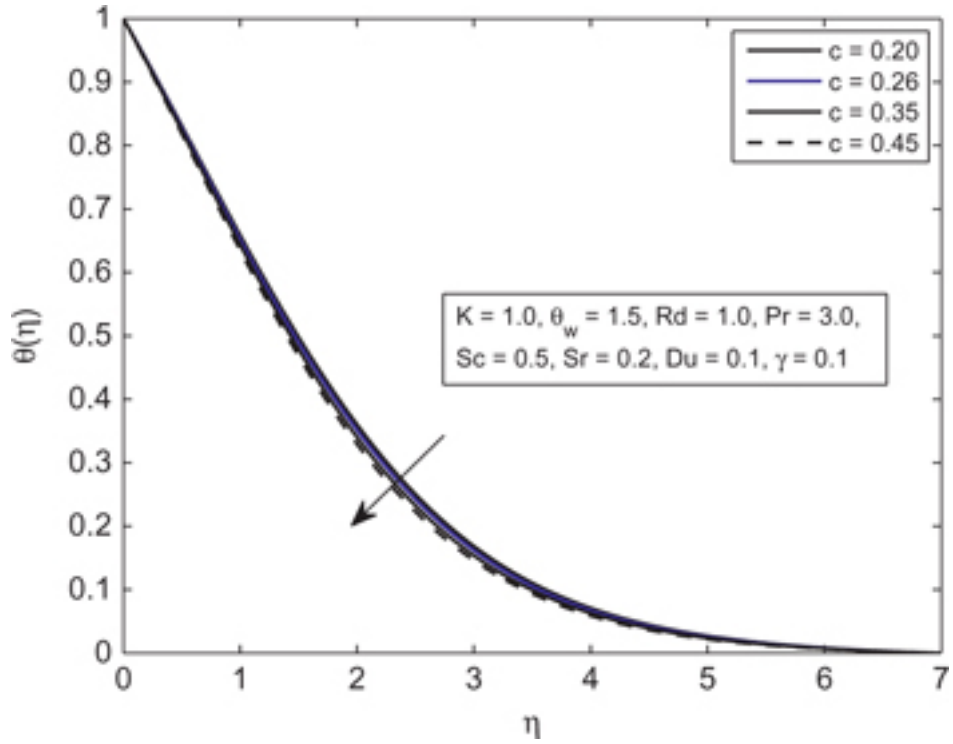

Figure 8: Influence of c on θ.

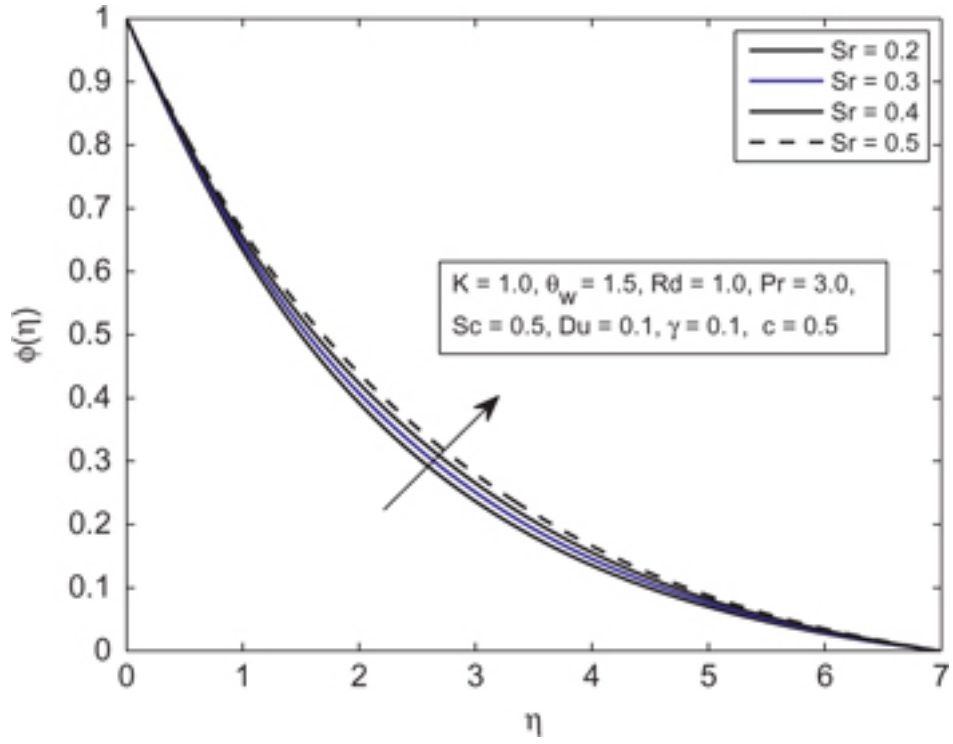

Figure 9: Influence of Sr on ϕ.

Brought to you by | University of Sussex Library
Authenticated
Download Date | 3/1/17 5:03 PM

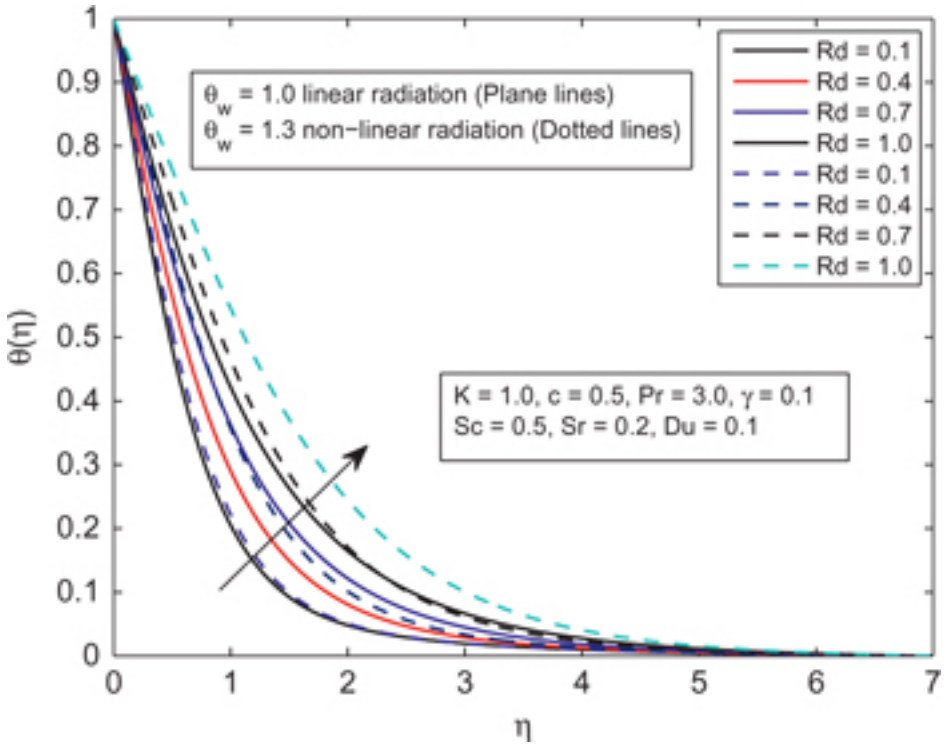

Figure 10: Influence of Rd on θ.

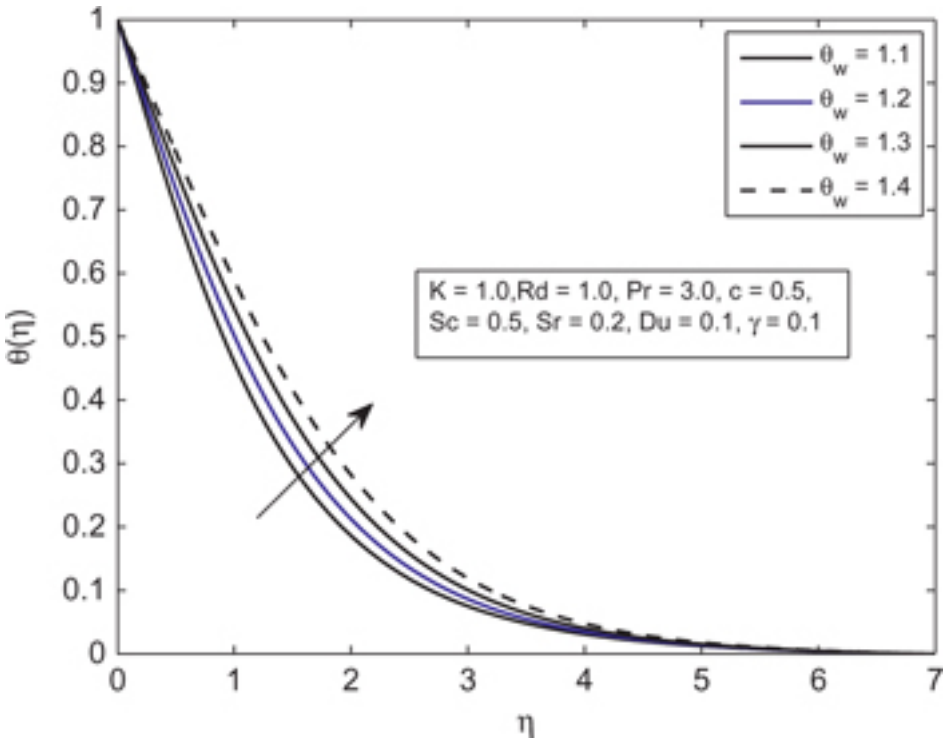

Figure 11: Influence of θ_w on θ.

An opposite response of chemical reaction parameter γ on temperature and concentration profile is noticed in Figure 12 and Figure 13 where temperature increases and concentration profile decreases for increasing value of γ. To see the variation in temperature and concentration against increasing value of Prandtl number Pr, Figure 14 and Figure 15 are plotted. It is observed that for increasing value of Prandtl number there is a thinner temperature boundary layer thickness. Fluids having larger Prandtl number results lower thermal diffusivity, and hence temperature decreases and concentration increases. The variation of Sc on temperature and mass transfer is shown in Figure 16 and Figure 17. From these figures it is noticed that the concentration boundary layer and hence concentration field $\phi(\eta)$ are reduced with the increment of Sc. This is due to the fact

Brought to you by | University of Sussex Library
Authenticated
Download Date | 3/1/17 5:03 PM

that *Sc* is inversely proportional to diffusion coefficient. As increase in diffusion coefficient decreases the mass transfer rate and hence increase in *Sc* results decrease in the concentration field and increase in temperature.

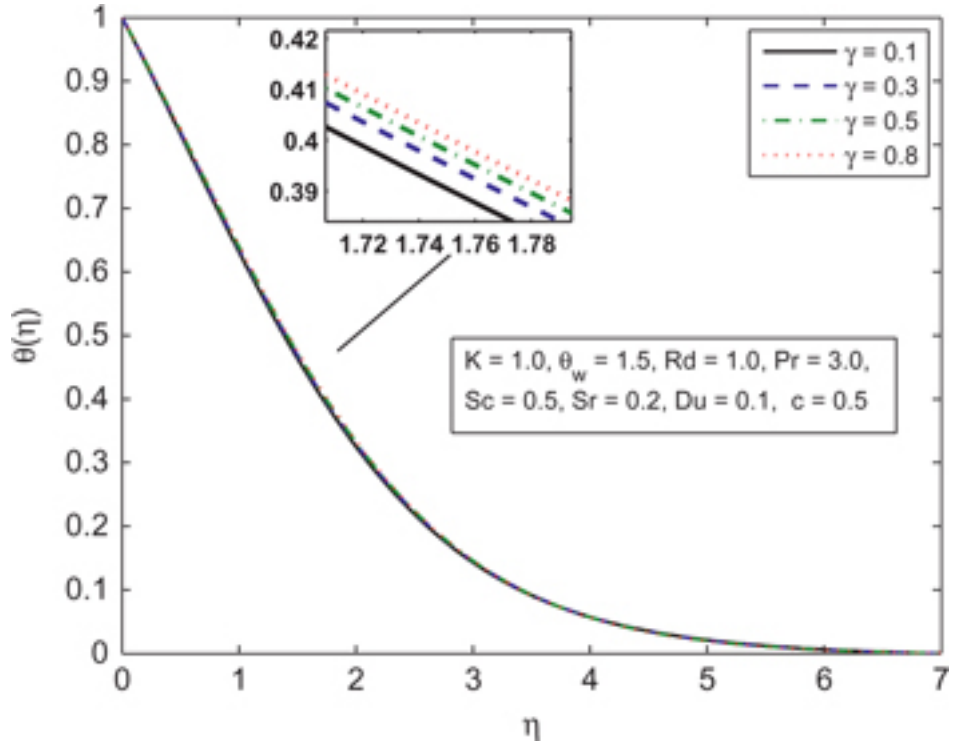

Figure 12: Influence of γ on θ.

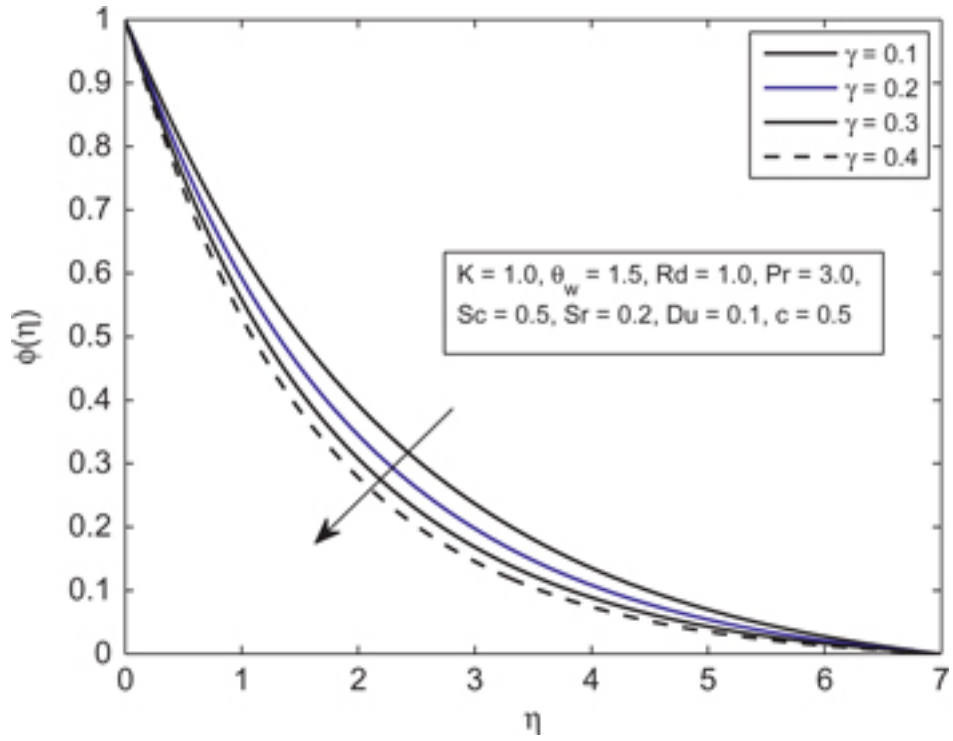

Figure 13: Influence of γ on ϕ.

Brought to you by | University of Sussex Library
Authenticated
Download Date | 3/1/17 5:03 PM

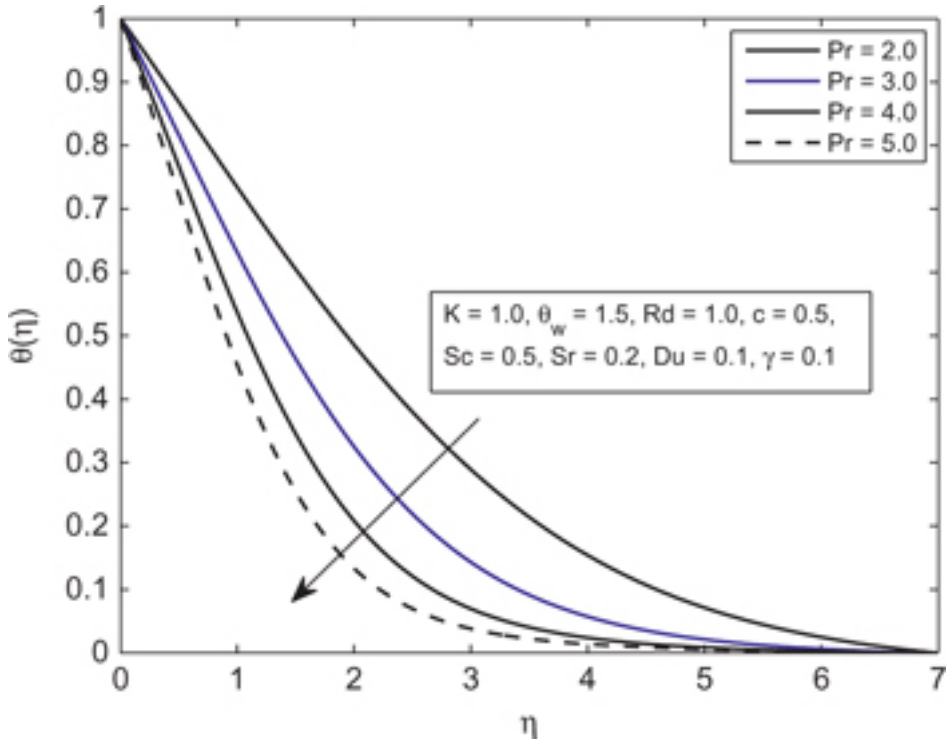

Figure 14: Influence of Pr on θ.

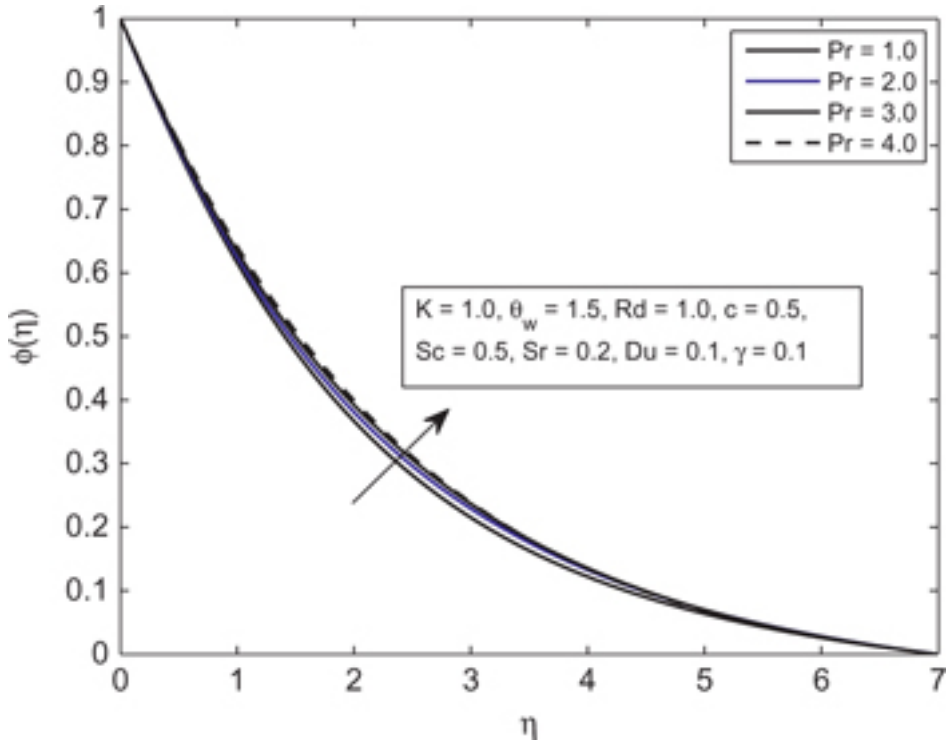

Figure 15: Influence of Pr on ϕ.

Brought to you by | University of Sussex Library
Authenticated
Download Date | 3/1/17 5:03 PM

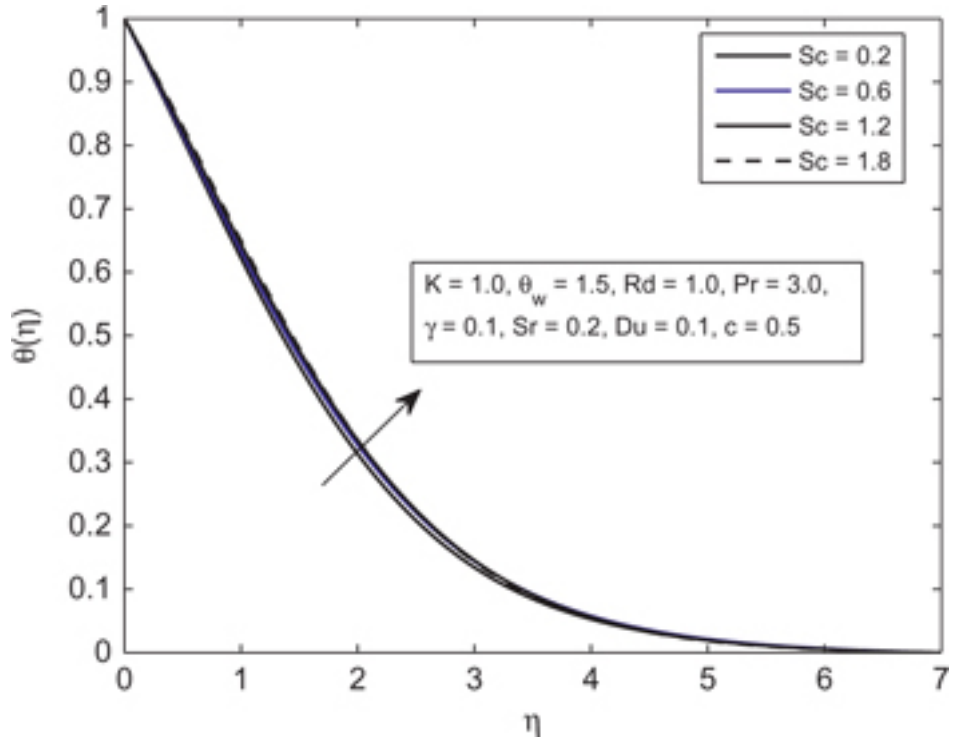

Figure 16: Influence of Sc on θ.

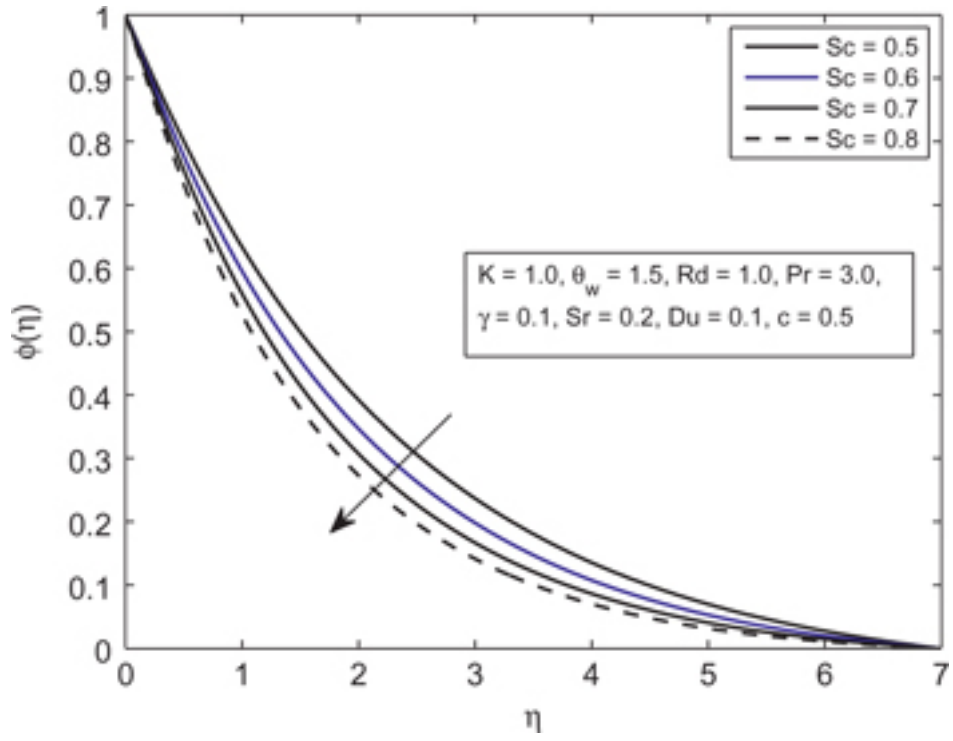

Figure 17: Influence of Sc on ϕ.

Figure 18 and Figure 19 depict the variation of Du on temperature and concentration profiles against η. From the graph it is observed that there is a considerable increase in temperature with the increase in Dufour number. This happens because Dufour number is directly proportional to the mass diffusion coefficient. Higher the mass diffusion coefficient implies high Dufour number and hence increase in Dufour number may increase in temperature and decrease in concentration.

Brought to you by | University of Sussex Library
Authenticated
Download Date | 3/1/17 5:03 PM

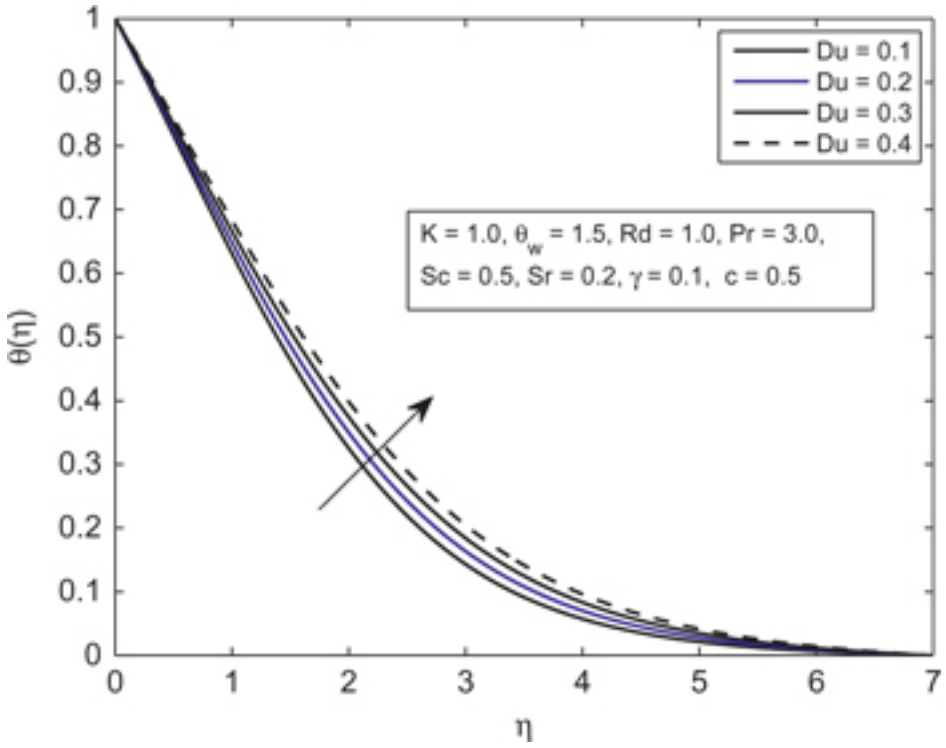

Figure 18: Influence of Du on θ.

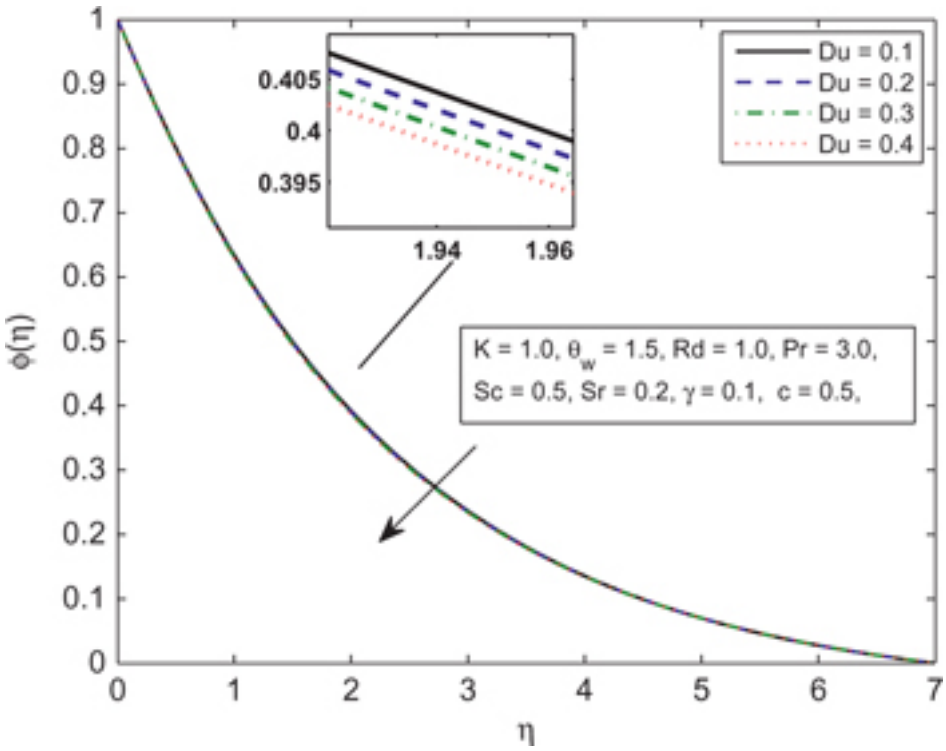

Figure 19: Influence of Du on ϕ.

In Table 1, a comparison of the present result with the previously published work is shown to validate our MATLAB code for various values of K, c and Pr. Results are found in a very good agreement. Numerical results of Local Nusselt number $\theta'(0)$ and Local Sherwood number $\phi'(0)$ for various values of different parameters are tabulated in Table 2. From the table, it is observed that rate of heat flux decreases for the increasing values of Deborah number K, temperature ratio parameter θ_w, thermal radiation parameter Rd, Schmidt number Sc, chemical reaction parameter γ and Dufour number Du. An increment is observed in the rate of heat flux for Prandtl number Pr, stretching ratio parameter c and Soret number Sr. Similarly Deborah number K, Prandtl number Pr, Soret number Sr, has decreasing effect on rate of mass transfer where as it increases for temperature

Brought to you by | University of Sussex Library
Authenticated
Download Date | 3/1/17 5:03 PM

ratio parameter θ_w, thermal radiation parameter Rd, stretching ratio parameter c, Schmidt number Sc, chemical reaction parameter γ and Dufour number Du.

Table 1: Comparison of wall temperature gradient $-\theta'(0)$ with Mushtaq et al. (2016b) for different values of K, c, Pr, Rd and θ_w.

K	c	Pr	$Rd = 0$ $\theta_w = 0$ **Mushtaq et al. (2016b))**	**Present**	$Rd = 1.0$ $\theta_w = 0$ **Mushtaq et al. (2016b))**	**Present**	$\theta_w = 1.1$ **Mushtaq et al. (2016b))**	**Present**	$\theta_w = 1.5$ **Mushtaq et al. (2016b))**	**Present**
1	0.5	2	1.01695	1.0169493	0.61177	0.6127148	0.53932	0.5395022	0.31686	0.3170918
		4	1.60165	1.6016506	1.01695	1.0169493	0.90348	0.9034844	0.55107	0.5510692
		7	2.24393	2.2439298	1.47271	1.4727082	1.31435	1.3143535	0.82083	0.8208336
		10	2.75508	2.7550740	1.83692	1.8369216	1.64284	1.6428361	1.03739	1.0373929
1	0	7	1.82603	1.8260260	1.20254	1.2025347	1.07372	1.0737145	0.67255	0.6725491
	0.3		2.09403	2.0940290	1.37824	1.3782398	1.23051	1.2305095	0.77013	0.7701323
	0.6		2.31293	2.3129240	1.51544	1.5154397	1.35219	1.3609931	0.84341	0.8434082
	1		2.55918	2.5591800	1.66440	1.6644187	1.48361	1.4836290	0.92038	0.9204030
0	0.5	7	2.35436	2.3543502	1.59321	1.5922506	1.42760	1.4275931	0.91088	0.9108748
0.5			2.29665	2.2966491	1.53021	1.5302076	1.36840	1.3684014	0.86380	0.8638003
1.0			2.24393	2.2439299	1.47271	1.4727082	1.31435	1.3143533	0.82083	0.8208334
1.5			2.19501	2.1950047	1.41998	1.4200796	1.26482	1.2649215	0.78170	0.7818260

Table 2: Numerical values of Local Nusselt number and Sherwood number.

K	θ_w	Rd	Pr	c	Sc	Sr	γ	Du	$-Nu_x Re_x^{-1/2}$	$-Sh_x Re_x^{-1/2}$
1.0	1.5	1	3.0	0.5	0.5	0.2	0.1	0.1	0.4082868	0.4226744
0.3									0.4743321	0.4635263
0.5									0.4531681	0.4493846
0.7									0.4338882	0.4374355
	1.1								0.6163549	0.3988861
	1.2								0.5397133	0.4062803
	1.3								0.4798611	0.4126387
		0.3							0.7142888	0.3936696
		0.6							0.5286367	0.4112719
		0.9							0.4313309	0.4204711
			1.5						0.2405017	0.4360473
			2.0						0.2958701	0.4314295
			2.5						0.3525910	0.4269351
				0.2					0.3753595	0.4029605
				0.35					0.3933766	0.4136870
				0.5					0.4082868	0.4226744
					0.2				0.4195913	0.2551274
					0.3				0.4155576	0.3118737
					0.4				0.4117984	0.3678961
						0.3			0.4089533	0.4123949
						0.4			0.4096215	0.4020679
						0.5			0.4102916	0.3916934
							0.2		0.4042825	0.4884968
							0.3		0.4008497	0.5455379
							0.4		0.3978162	0.5963516
								0.2	0.3878539	0.4242541
								0.3	0.3672307	0.4258499
								0.4	0.3464141	0.4274624

Brought to you by | University of Sussex Library
Authenticated
Download Date | 3/1/17 5:03 PM

5 Concluding remarks

This study reveals the influence of non-linear thermal radiation of electrically conducting upper convected Maxwell fluid over a bi-directional stretching surface. Effect of Soret and Dofour in the presence of homogenous chemical reaction are also taken into account. Non-linear differential equations are solved numerically by using bvp4c built-in MATLAB function. The main features of the study are highlighted as

- UCM fluids have lower boundary layer thickness as compared to Newtonian fluid.
- The present results are valid for both, the linear radiation ($\theta_w = 1.0$) as well as for non-linear ($\theta_w > 1$) radiation.
- Soret and Dufour have opposite effects on the concentration profile.
- Schmidt number have opposite relation with temperature and concentration profile.
- An increase in thermal boundary layer thickness is observed in temperature profile. This increase in temperature is higher for non-linear radiation ($\theta_w = 1.3$) as compared to linear radiation ($\theta_w = 1.0$).

Funding

Korea Institute of Energy Technology Evaluation and Planning (KETEP), (Grant/Award Number: '20132010101780').

Nomenclature

a, b Dimensional constants
C Concentration of fluid
c Stretching ratio parameter
c_p Specific heat
C_s Concentration susceptibility
C_w Concentration on wall
C_∞ Ambient concentration
D_m Mass diffusivity
Du Dufour number
f', g' Dimensionless velocities
j_w Mass flux
κ Thermal conductivity
k_T Thermal diffusion ratio
K_1 Chemical reaction coefficient
Nu_x Nusselt number
Pr Prandtl number
q_r Radiative heat flux
q_w Surface heat flux
Rd Thermal radiation parameter
Re Reynold number
Sc Schmidt number
Sh_x Sherwood number
Sr Soret number
T Temperature of fluid

Brought to you by | University of Sussex Library
Authenticated
Download Date | 3/1/17 5:03 PM

T_m Mean fluid temperature
T_w Wall temperature
T_∞ Ambient temperature
(u, v, w) Velocity components
$U_w(x)$ Stretching velocity along x-axis
$V_w(y)$ Stretching velocity along y-axis
α_m Thermal diffusivity
ρ Density of fluid
σ^* Steffan-Boltzman constant
λ_1 Fluid relaxation time
ν Kinematic viscosity
θ Dimensionless temperature
γ Chemical reaction parameter
η Similarity variable
θ_w Temperature ratio parameter
ϕ Dimensionless concentration

References

Abel, M.S., V. Jagadish, M. Tawade, and M. Mahantesh. 2012. "MHD flow and heat transfer for the upper-convected maxwell fluid over a stretching sheet." *Meccanica* 47 : 385–393.

Ali, N., S.U. Khan, M. Sajid, and Z. Abbas. 2016. "Flow and heat transfer of hydromagnetic Oldroyd-B fluid in a channel with stretching walls." *Nonlinear Engineering* 5 (2): 73–79.

Awais, M., T. Hayat, A. Alsaedi, and S. Asghar. 2014. "Time-dependent three-dimensional boundary layer flow of a Maxwell fluid." *Compputers and Fluids* 91 : 21–27.

Beg, O.A., R. Bhargava, S. Rawat, H.S. Takhar, and T.A. Beg. 2007. "A study of steady buoyancy-driven dissipative micropolar free convection heat and mass transfer in a darcian porous regime with chemical reaction." *Nonlinear Analysis: Modelling and Control* 12 : 157–180.

Beg, O.A., M.M. Rashidi, M. Keimanesh, and T.A. Beg. 2013. "Semi-numerical modelling of chemically-frozen combusting buoyancy-driven boundary layer flow along an inclined surface." *International Journal of Applied Mathematics and Mechanics* 9 : 1–16.

Bhattacharyya, K., T. Hayat, and A. Alsaedi. 2014. "Dual solutions in boundary layer flow of Maxwell fluid over a porous shrinking sheet." *Chinese Physics B* 23 : 124701.

Chapman, S., and T.G. Cowling. 1940. *The Mathematical Theory of Non-Uniform Gases*. Cambridge: Cambridge University Press.

Chia, E.S. 2006. *A Chemical Reaction Engineering Perspective of Polymer Electrolyte Membrane Fuel Cells*. Princeton, NJ: Chemical Engineering, Princeton University.

Eckert, E.R.G., and R.M. Drake. 1972. *Analysis Heat Mass Transfer*. New York: McGraw-Hill.

Hayat, T., M.B. Ashraf, A. Alsaedi, and M.S. Alhuthali. 2015. "Soret and Dufour effects in three-dimensional flow of maxwell fluid with chemical reaction and convective condition." *International Journal of Numerical Methods for Heat and Fluid Flow* 25 (1): 14.

Hayat, T., M. Ijaz Khan, M. Waqas, A. Alsaedi, and T. Yasmeen. 2016a. "Diffusion of chemically reactive species in third grade flow over an exponentially stretching sheet considering magnetic field effects." *Chinese Journal of Chemical Engineering*. DOI:10.1016/j.cjche.2016.06.008.

Hayat, T., R. Iqbal, A. Tanveer, and A. Alsaedi. 2016a. "Soret and Dufour effects in MHD peristalsis of pseudoplastic nanofluid with chemical reaction." *Journal of Molecular Liquid* 220 : 693–706.

Hayat, T., R. Iqbal, A. Tanveer, and A. Alsaedi. 2016b. "Influence of convective conditions in radiative peristaltic flow of pseudoplastic nanofluid in a tapered asymmetric channel." *Journal of Magnetism and Magnetic Materials* 408 : 168–176.

Hayat, T., M. Shafique, A. Tanveer, and A. Alsaedi. 2016b. "Radiative peristaltic flow of jeffrey nanofluid with slip conditions and joule heating." *Plos ONE* 11 (2): 0148002.

Hirshfelder, J.O., C.F. Curtis, and R.B. Bird. 1954. *Molecular Theory of Gases and Liquids*, 1249. New York: John Wiley.

Kasmani, R.M., S. Sivasankaran, M. Bhuvaneswari, and Z. Siri. 2016. "Effect of chemical reaction on convective heat transfer of boundary layer flow in nanofluid over a wedge with heat generation/absorption and suction." *Journal of Applied Fluid Mechanics* 9 : 379–388.

Liu, I.C., and H.I. Andersson. 2008. "Heat transfer over a bidirectional stretching sheet with variable thermal conditions." *International Journal of Heat and Mass Transfer* 51 : 4018–4024.

Makinde, O.D., and P.O. Olanrewaju. 2011. "Unsteady mixed convection with Soret and Dufour effects past a porous plate moving through a binary mixture of chemically reacting fluid." *Chemical Engineering Communications* 198 : 920–938.

Merkin, J.H., and T. Mahmood. 1998. "The convective flow on a reacting surface in a porous medium." *Transport Phenomena in Porous Media* 33 : 279–293.

Mingchun, L.I., Z. Zhongliang, Y. Jing, L. Jiatao, and W. Yusheng. 2013. "The Soret and Dufour effects in non-thermal equilibrium packed beds with forced convection and endothermic reactions." *Chinese Journal of Chemical Engineering* 21 : 867–875.

Brought to you by | University of Sussex Library
Authenticated
Download Date | 3/1/17 5:03 PM

Mushtaq, A., S. Abbasbandy, M. Mustafa, T. Hayat, and A. Alsaedi. 2016a. "Numerical solution for Sakiadis flow of upper-convected maxwell fluid using Cattaneo-Christov heat flux model." *AIP Advances* 6 : 015208.

Mushtaq, A., M. Mustafa, T. Hayat, and A. Alsaedi. 2016b. "A numerical study for three-dimensional viscoelastic flow inspired by non-linear radiative heat flux." *International Journal Non-Linear Mechanics* 79 : 83–87.

Ojjela, O., and N.N. Kumar. 2016. "Unsteady MHD mixed convection flow of chemically reacting micropolar fluid between porous parallel plates with Soret and Dufour effects." *Journal of Engineering* 13 : 2016.

Ramzan, M., and M. Bilal. 2015. "Time dependent MHD nano-second grade fluid flow induced by permeable vertical sheet with mixed convection and thermal radiation." *Plos ONE* 10 (5): 0124929.

Ramzan, M., and M. Bilal. 2016. "Three-dimensional flow of an elastico-viscous nanofluid with chemical reaction and magneticfield effects." *Journal of Molecular Liquid* 215 : 212–220.

Ramzan, M., M. Bilal, U. Farooq, and J.D. Chung. 2016. "Mixed convective radiative flow of second grade nanofluid with convective boundary conditions: an optimal solution." *Results in Physica* 6 : 796–804.

Reddy, B.N., S.V.K. Varma, and B.R. Kumar. 2016. "Soret and Dufour effects on MHD boundary layer flow past a stretching plate." *Intternational Journal of Engineering Research Africa* 22 : 22–32.

Ren, Q., and C.L. Chan. 2016. "Numerical study of double-diffusive convection in a vertical cavity with Soret and Dufour effects by Lattice Boltzmann method on GPU." *International Journal of Heat and Mass Transfer* 93 : 538–553.

Sadeghya, K., H. Hajibeygi, and S.M. Taghavia. 2006. "Stagnation-point flow of upper-convected Maxwell fluids." *International Journal of Non-Linear Mechanics* 41 : 1242–1247.

Steinfeld, S., and R. Palumbo. 2001. "Solar thermochemical process technology, encyclopedia of physical science technology." *R. A. Meyers Academic Press* 15 : 237–256.

Uddin, M.J., O.A. Beg, A. Aziz, and A.I.M. Ismail. 2015. "Group analysis of free convection flow of a magnetic nanofluid with chemical reaction." *Mathematical Problems in Engineering* 2015 : 1–11. DOI:10.1155/2015/621503.

Brought to you by | University of Sussex Library
Authenticated
Download Date | 3/1/17 5:03 PM